ACS APPLIED MATERIALS & INTERFACES

Letter

www.acsami.org

Robust Superamphiphobic Film from Electrospun TiO_2 Nanostructures

V. Anand Ganesh,[†,‡,§,⊥] Saman Safari Dinachali,[†,‡] A. Sreekumaran Nair,[*,#] and Seeram Ramakrishna[†,§]

[†]Department of Mechanical Engineering, [§]Centre for Nanofibers & Nanotechnology, Nanoscience and Nanotechnology Initiative, [⊥]Solar Energy Research Institute of Singapore, National University of Singapore, Singapore

[‡]Institute of Materials Research and Engineering, Agency for Science, Technology and Research, 3 Research Link, Singapore 117602

[#]Amrita Centre for Nanosciences & Molecular Medicine, Amrita Institute of Medical Sciences, Amrita Vishwa Vidyapeetham, AIMS Ponnekkara P.O., Kochi-682041, Kerala, India

Supporting Information

ABSTRACT: Rice-shaped TiO_2 nanostructures are fabricated by electrospinning for creating a robust superamphiphobic coating on glass substrates. The as-fabricated TiO_2 nanostructures (sintered at 500 °C) are superhydrophilic in nature which upon silanization turn into superamphiphobic surface with surface contact angle (SCA) values achieved using water (surface tension, γ = 72.1 mN/m) and hexadecane (surface tension, γ = 27.5 mN/m) being 166° and 138.5°, respectively. The contact angle hysteresis for the droplet of water and hexadecane are measured to be 2 and 12°, respectively. Thus, we have successfully fabricated superior self-cleaning coatings that possess exceptional superamphiphobic property by employing a simple, cost-effective, and scalable technique called electrospinning. Furthermore, the coating showed good mechanical and thermal stability with strong adherence to glass surface, thus revealing the potential for real applications.

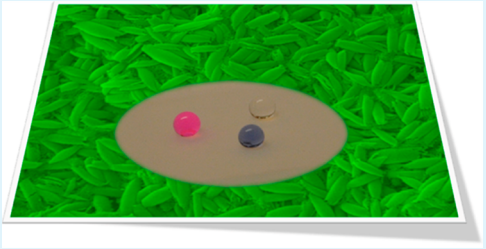

KEYWORDS: *superamphiphobicity, electrospinning, rice-shaped TiO_2, surface contact angle, contact angle hysteresis and self-cleaning*

One of the major objectives in surface coating research is to fabricate self-cleaning surfaces because of their numerous applications including anti-misting, anti-microbial, corrosion resistance, oil-repellency, etc.[1−7] Self-cleaning coatings can be classified into two categories: superhydrophilic[8−12] and superhydrophobic coatings.[13−23] Superhydrophilic surfaces clean themselves by the sheeting effect of water and also by breaking down the complex organic substances into carbon dioxide and water − the photocatalytic effect.[24−28] In superhydrophobic coatings, the air pockets that get trapped between the substrate with nanostructures and water (Cassie's state) facilitate the water to form spherical droplets and enable the droplets to roll-off easily across the surface taking away the dirt and other pollutants.[29] Nature has given us many self-cleaning superhydrophobic surfaces ranging from lotus/rice leaves, bird's feathers, butterfly wings, water strider's legs, etc., and by mimicking their surface morphology, several self-cleaning superhydrophobic surfaces have been developed in the recent past.[30−32] Nevertheless, to have an effective self-cleaning action, the coating should be able to repel organic liquids besides water. To address this need, researchers have recently developed a new type of coating that can repel both water and organic liquids known as superamphiphobic coatings.[33−37] The key criteria to achieve the phenomenon of superamphiphobicity are not yet clearly defined; however, lower surface energy and surface roughness are the necessary factors for oil/water repellency.[38,39] There are only a few studies on designing superamphiphobic surfaces, because of its difficulty to fabricate rough surfaces, which involve surface over hangs and re-entrant geometry.[40−49]

Here we describe a simple and scalable way to fabricate a superior self-cleaning coating that exhibits exceptional superamphiphobic property. We have employed electrospinning technique to fabricate a coating consisting of porous rice-shaped TiO_2 nanostructures, which upon fluorinated silane treatment turns into superamphiphobic surface. The surface contact angle achieved using water (γ = 72.1 mN/m) and hexadecane (γ = 27.5 mN/m) were 166° ± 0.9 and 138.5° ± 1, respectively. The contact angle hysteresis for a droplet of water and hexadecane were measured to be 2 and 12°, respectively.

The rice-shaped TiO_2 obtained from electrospun PVAc-TiO_2 (PVAc − polyvinly acetate) composite nanofibers was used to fabricate superamphiphobic coating (Scheme 1). A thick layer (2 μm) of electrospun PVAc-TiO_2 composite nanofibers (average fiber diameter: 125 ± 15 nm) were deposited on the cleaned glass substrate (Figure 1). The coated glass samples were then sintered at 500 °C for 1 h (in air medium) with a ramping rate of 5 °C per min. During the heat treatment process, the continuous fiber morphology breaks down resulting in the formation of rice-shaped TiO_2 nanostructures. We have already established that the uniquely shaped

Received: November 21, 2012
Accepted: February 21, 2013
Published: February 21, 2013

Scheme 1. Fabrication of Superamphiphobic Coating: Process Flow Chart (this schematic is not drawn to scale)

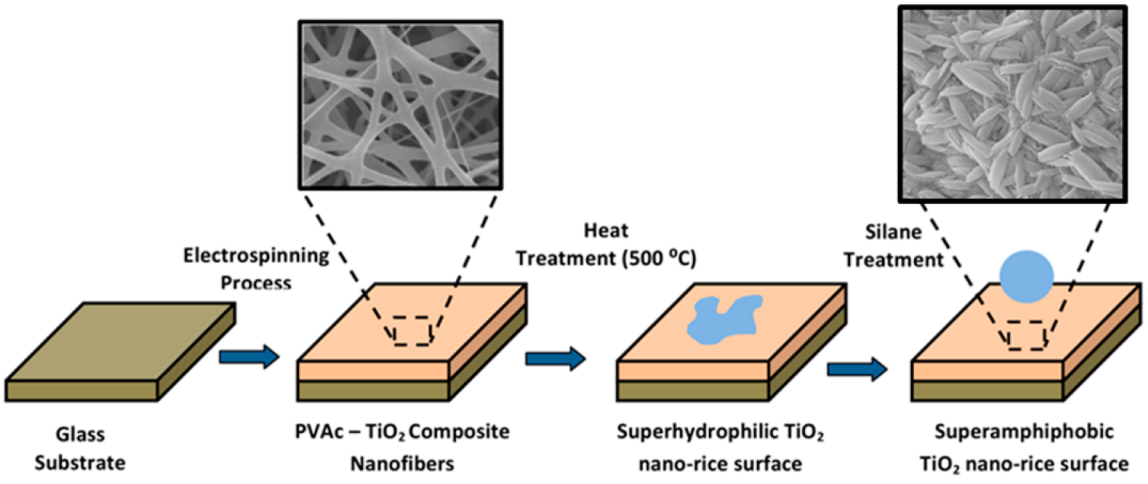

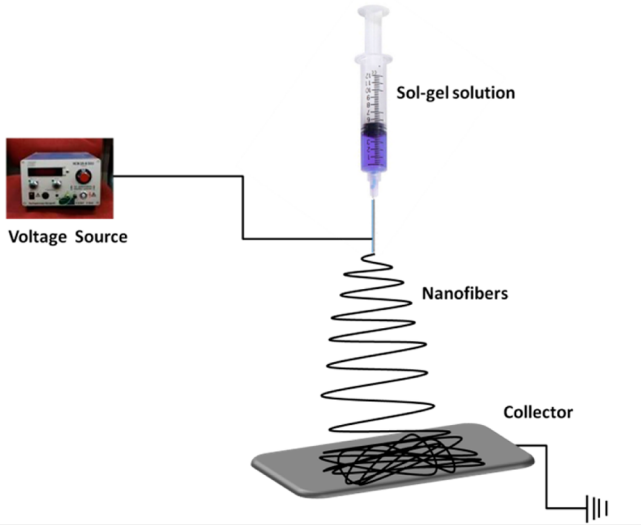

Figure 1. Schematic diagram of the electrospinning set-up.

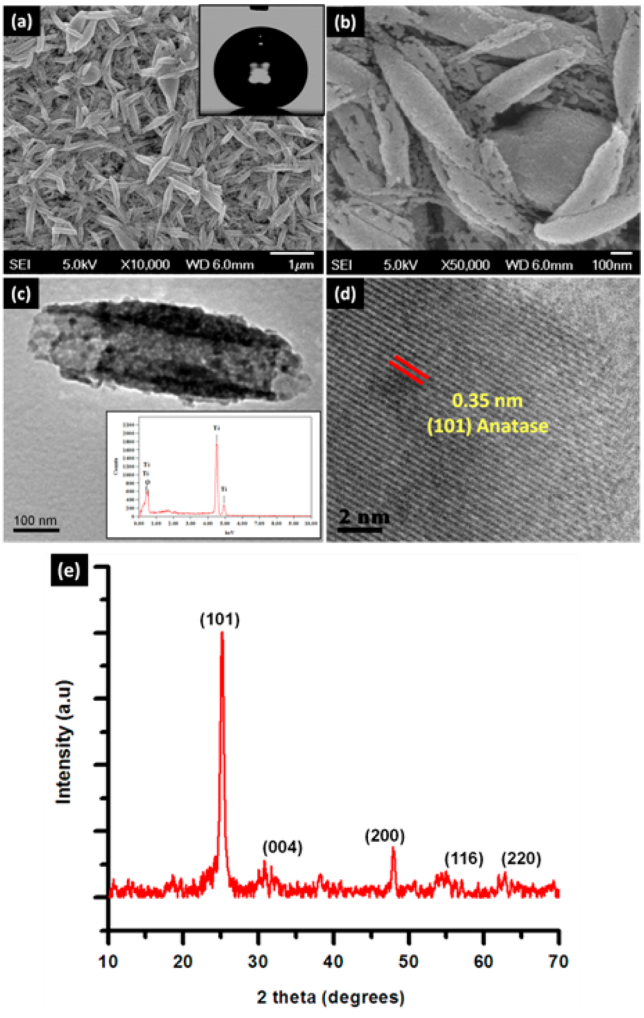

Figure 2. (a, b) SEM images (low and high magnification) of the TiO_2-coated samples (inset: interaction of water droplet (1 μL) with the coated surface. WCA: 166°); (c) TEM image of a single nano-rice structure (inset: EDS spectrum of the TiO_2 coated sample); (d) the lattice-resolved image; (e) XRD of the TiO_2-coated sample sintered at 500 °C.

nanostructures were the result of microscale phase separation between the PVAc and the TiO_2 occurring during the sintering process (note that if we use PVP, polyvinylpyrrolidone, instead of PVAc, the result will always be continuous TiO_2 nanofibers and not the rice-shaped TiO_2).[50,51] Electrospinning is essential to get the rice-shaped structures as the same evolved from the smooth electrospun fibers were interconnected and well-defined in size, shape, and porosity.[50−54] The degradation of the polymer (PVAc) from the PVAc-TiO_2 composite imparts high porosity (and hence surface roughness) to the TiO_2 nanostructures (BET surface area of ∼60 m^2/g).[51] Images a and b in Figure 2 show the low- and high-magnification SEM images of the electrospun-TiO_2 coated sample, exhibiting a uniform distribution of porous rice-shaped nanostructures. Figure 2c shows the TEM image of a single nano-rice structure. From the image, it could be observed that a single TiO_2 nanostructure is made of numerous spherical particles with an average diameter of 12−15 nm. The TGA analysis (Figure S1 in the Supporting Information) and the EDS spectrum (inset in Figure 2c) confirmed that after the heat treatment process, the sample was free from polymer or other organics.[55,56] The lattice-resolved TEM image (d spacing = 0.35 nm, Figure 2d) and XRD measurement (Figure 2e) further confirmed that the coating contained particles of anatase TiO_2.

dx.doi.org/10.1021/am302790d | ACS Appl. Mater. Interfaces 2013, 5, 1527−1532

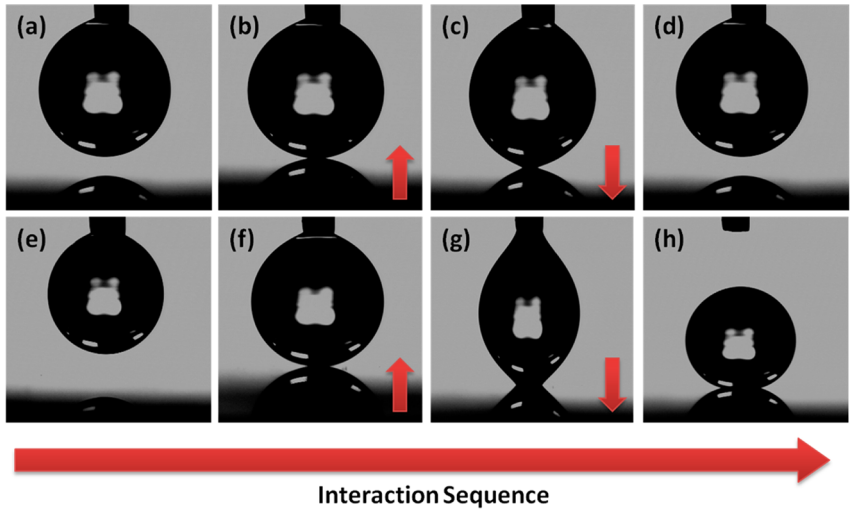

Figure 3. (a–d) shows the interaction of water droplet (1μL) with superamphiphobic surface; (e–h) shows the interaction of glycerol droplet (1 μL) with the superamphiphobic surface (SCA: 158.3°).

Table 1. Surface Contact Angle and Roll-off Angle Measurements of Liquids with Different Surface Tension on a Superamphiphobic Glass Substrate

S. No	liquid	surface tension (mN/m)	surface contact angle (deg)	advancing (θ_a)/ receding (θ_r) contact angles (deg)	contact angle hysteresis (CAH) (θ_a–θ_r) (deg)	roll-off angle (RA)/sliding angle (SA) (deg)
1	water	72.1	166 ± 0.9	169/167	2	1 ± 1 (RA)
2	glycerol	64	158.3 ± 0.7	160/156	4	6 ± 1 (RA)
3	di-iodomethane	50.9	155.7 ± 0.8	157/150	7	9 ± 1 (RA)
4	ethylene glycol	47.3	152.6 ± 1.1	155/147	8	9 ± 1 (RA)
5	vegetable oil	34.5	147.3 ± 1	153/142	11	13 ± 1 (SA)
6	hexadecane	27.4	138.5 ± 1	147/135	12	15 ± 1 (SA)
7	dodecane	25.3	127.6 ± 0.7	138/124	14	15 ± 2 (SA)

The rice-shaped TiO_2-coated samples (thickness of the coating: 375 ± 10 nm) exhibited superhydrophilic property (water contact angle, WCA approx. equal to 0).[57] In order to reduce the surface energy of the superhydrophilic TiO_2 nanostructures, the samples were coated with fluorinated silane for 3 h using chemical vapor deposition (CVD) process (Figure S2 in the Supporting Information). The high porosity and hence the large surface area (and surface roughness) of the nanostructures ensured sufficient intake of flourosilane upon silane treatment. After silanization, the coating exhibited superamphiphobic property with contact angle as high as 166 and 158.3°, respectively, were achieved for 1 μL droplet of water and glycerol (Figure 3). It must also be noted that the ricelike structures were actually made of very small spherical particles of 12–15 nm sizes (see TEM image) and the innumerable number of such small fluorinated particles prevent water/oil from wetting the surfaces resulting in superamphiphobicity. Because of the extremely low adhesion and surface energy, it was very tough to deposit water droplet on the coating. The water droplet (2 μL) immediately started rolling-off when it comes in contact with the coated surface.

The surface contact angle (SCA), roll-off angle, and the advancing (θ_a)/receding angle (θ_r) were measured for several liquids with different surface tension (such as water, glycerol, di-iodomethane, ethylene glycol, vegetable oil, dodecane and hexadecane) by using a "tilting base surface contact angle measurement set-up" and the contact angle hysteresis (CAH) was calculated by taking the difference of advancing and receding angles (Table 1, Figure 4, and Figure S3 in the Supporting Information). The CAH achieved for water, ethylene glycol and hexadecane were 2, 8, and 12°, respectively.

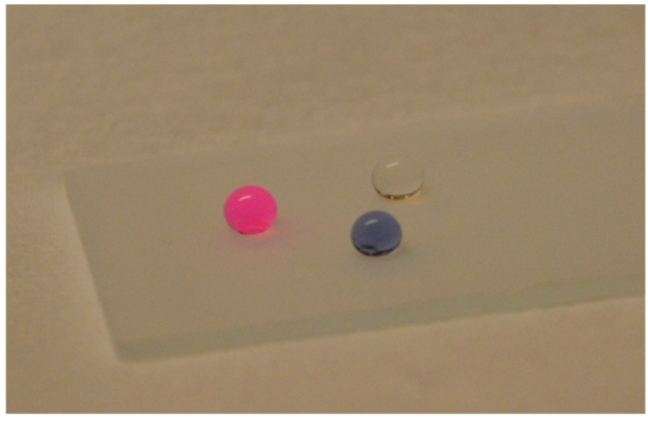

Figure 4. Photograph of water (blue; dyed with trypan blue dye), glycerol (pink; dyed with rhodamine B), and ethylene glycol (colorless) droplets on the superamphiphobic surface.

To analyze the mechanical stability of the coated samples, indentation studies were carried out using a nanoindentation setup equipped with a Berkovick tip. The measurements were conducted at five different places of the coated sample and the average hardness & Young's modulus values of the coating were measured to be 0.12 GPa and 3.26 GPa, respectively (refer to Table S4 in the Supporting Information).

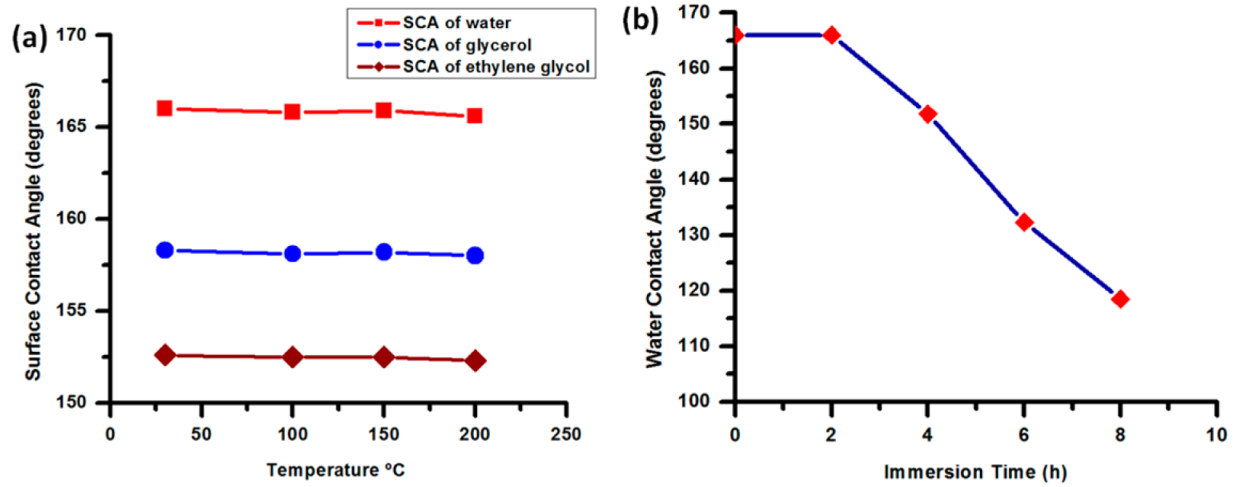

Figure 5. (a) Surface contact angle values made by water, glycerol and ethylene glycol droplets on the superamphiphobic surface after heat treatment for 2 h at different temperatures; (b) WCA values made by the water droplets on the TiO_2-coated surface for different immersion time in hot aqueous ethanol solution.

Temperature stability test was conducted on the coated sample by heating the sample at different temperatures (100, 150, and 200 °C) for 2 h (note that the flash temperature of the flourosilane is >200 ^{0}C). The results indicated that values of surface contact angles and roll-off angles remained similar after the heat treatment process (Figure 5a). To study the behavior of the superamphiphobic coating towards organic solvents, the coated samples were kept immeresed in a hot aqueous solution of ethanol (60%) heated at 80 °C for different time intervals (2, 4, 6, and 8 h). It was observed that the water contact angle (WCA) value remained unchanged for 2 h (WCA: 166°) and started dropping for longer time intervals (Table 2, Figure 5b).

Table 2. WCA Measurements of the Superamphiphobic Coated Samples When Kept Immersed in Hot Aqueous Solution of Ethanol at Different Time Intervals

sample	immersion time in hot aqueous ethanol solution (h)	water contact angle (WCA) (deg)
1	0	166 ± 0.9
2	2	166 ± 0.9
3	4	151.8 ± 0.7
4	6	132.3 ± 1
5	8	118.5 ± 0.8

We believe that this could be because of the leaching of some of the physisorbed fluorosilane on TiO_2 surfaces (during the CVD process, some fluorosilane could also be loosely bound on the TiO_2 surfaces) into the hot ethanol upon prolonged treatment and hence there is a reduction in the WCA. Superamphiphobicity of the coating can be recovered by heating the TiO_2 coated sample to 500 °C for 1 h (ramping rate 5 °C per min) followed by fluorinated silane treatment.

A 90° peel-off test was conducted on the coated sample using an adhesion tape (3M scotch tape). The tape was peeled-off from the coated surface (test distance: 50 mm) by applying a fixed force of 5 ± 0.1 N. After the peel-off test, it was observed that the coating remained stable without forming any cracks/scratches on the surface (Figures S5 and S6 in the Supporting Information). The samples before and after peel-off test were imaged by SEM to check whether there was any change in the morphology of the nanostructures. Images in Figure S6 in the Supporting Information confirm that there were no changes even in micrometer scale regimes.

The coated samples were placed in an environment which was maintained at Standard Ambient Temperature and Pressure condition (temperature, 25 ± 2 °C; pressure, 0.986 atm., humidity, 40−60%).[58] SCA measurements for water, ethylene glycol and hexadecane were carried out on weekly basis (Table 3). The results indicated that the coating is

Table 3. SCA Measurements of the Superamphiphobic Coated Samples When Kept in SATP (Standard Ambient Temperature and Pressure) Conditions

sample	time duration (in weeks)	surface contact angle made by water droplet (SCA) (deg)	surface contact angle made by ethylene glycol droplet (SCA) (deg)	surface contact angle made by hexadecane droplet (SCA) (deg)
1	after 2 weeks	166 ± 0.9	152.6 ± 1.1	138 ± 0.7
2	after 4 weeks	166 ± 0.6	152.6 ± 0.7	138 ± 1
3	after 6 weeks	166 ± 0.7	152.6 ± 0.9	138 ± 1.1
4	after 8 weeks	166 ± 0.5	152.6 ± 0.6	138 ± 0.9

environmentally very stable and retained the superamphiphobic property (the samples are still under examination and measurements are still being carried out every week).

To summarize, we have fabricated a robust superamphiphobic coatings on the glass substrate from electrospun TiO_2 rice-shaped nanostructures. The electrospun PVAc-TiO_2 composite nanofibers on sintering resulted in the formation of porous superhydrophilic rice shaped nanostructures which upon silanization turn into superamphiphobic surface. The synthesized coatings were characterized using SEM, EDS, XRD, TEM and TGA. The superamphiphobic property of the coatings was studied. The results indicated that the porous electrospun anatase TiO_2 films were able to exhibit superamphiphobic property with surface contact angle values achieved for water (γ = 72.1 mN/m) and hexadecane (γ = 27.5 mN/m) were 166 and 138.5°, respectively. Furthermore, the coating showed exceptional mechanical and thermal stability with strong

adherence to the glass substrate thus revealing the potential for windows and other real time applications.

EXPERIMENTAL SECTION

Materials and Methods. Polyvinyl acetate (Sigma Aldrich, M_w = 500 000), *N,N*-dimethylacetamide (DMAc, 99.8%, GC Grade, Aldrich, Germany), (tridecafluoro-1,1,2,2-tetrahydrooctyl)-1-trichlorosilane (Alfa Aesar, 97%), acetic acid (99.7%, LAB-SCAN Analytical Sciences, Thailand), absolute ethanol (Fisher Scientific, 99.5%), ethylene glycol, glycerol, di-iodomethane, hexadecane, dodecane (all from Aldrich), vegetable oil, and de-ionized water were used without any further purification.

The sol-gel solution for the deposition of TiO_2 nanostructures on glass substrate was prepared as follows. About 1.2 g of polyvinyl acetate was added to 10 mL of *N,N*-dimethylacetamide (DMAc). This was followed by the addition of a TiO_2 sol prepared by mixing 2 mL of acetic acid and 1 mL of titanium(IV) isopropoxide. The prepared solution was stirred at room temperature for about 12 h to acquire sufficient viscosity for electrospinning.

Microscopic slide glass plates (24.4 mm × 76.2 mm × 1.2 mm) were thoroughly cleaned by ultra-sonication in de-ionized water, ethanol, acetone and isopropanol, respectively, for about 15 min each. To ensure that the glass slides were free from surface contaminants, they were cleaned with Piranha solution (3:7 by volume of 30% H_2O_2 and H_2SO_4) followed by rinsing in de-ionized water. The cleaned glass plates were dried in an oven at 80 ^{0}C.

The solution containing the TiO_2 precursor was loaded into the electrospinning machine (NANON, MECC- Japan). The washed and dried microscopic glass slides were then mounted on a flat collector wrapped with aluminium foil. The applied voltage was set to 30 kV and the distance between the needle (27G 1/2) tip and the static collector was set to 10 cm. The humidity level in the electrospinning chamber was maintained between 50 and 60%. The PVAc-TiO_2 precursor solution was electrospun on the glass substrates for 15 min with a flow rate of about 1 mL h^{-1} to deposit a uniform layer of PVAc-TiO_2 composite nanofibers on the glass substrate. The PVAc-TiO_2 composite nanofibers upon heat treatment process (500 ^{0}C for 1 h for polymer degradation) results in finely distributed porous rice-shaped TiO_2 nanostructures.

After the heat treatment (annealing) process, the porous TiO_2-coated glass samples were superhydrophilic in nature. In order to reduce the surface energy and to induce the superamphiphobic property into the superhydrophilic structures, the coated samples were put inside a desiccator along with a glass bottle containing 50 μL of fluorinated silane for 3 h under vacuum. The samples were then characterized by spectroscopy, microscopy, thermogravimetry, contact angle measurements, and durability tests.

Instrumentation. The samples for scanning electron microscopy (SEM) were gold sputtered and the images were captured using a field emission SEM instrument (FESEM, JEOL FESEM JSM-6700F) operated at 5 kV. The energy-dispersive X-ray spectroscopy (EDS) data were also obtained from the same machine.The thickness of the film was measured by a surface profiler (Alpha-Step IQ Surface Profiler). The contact angle measurements (static, advancing, receding, and roll-off angles) were carried out using a contact angle measurement setup (VCA optima contact angle equipment from AST Products) in static/dynamic sessile drop mode at room temperature. The surface contact angle values reported were the averages of at least five measurements made on different areas of the coated sample. Thermogravimetric analysis (TGA, TA Instruments Q100) was performed to study the degradation behavior of the sol-gel and formation of oxide. X-ray Diffraction (XRD) pattern was obtained using general area detector diffraction system (Bruker D8,GADDS-XRD). TEM images of the sintered rice-shaped nanostructures were taken by a high-resolution transmission electron microscope (HR-TEM, JEOL 3010 operated at 300 kV). The sample for the HR-TEM was prepared by dispersing the sintered TiO_2 powder (TiO_2 nanofibers were deposited on the aluminium foil and after sintering, the pure TiO_2 material was scraped-off from the aluminium foil) in methanol under sonication and then a drop of this suspension is allowed to dry on a carbon-coated copper grid. Hardness and modulus values of the coating were measured by nanoindentation set-up (Agilent Nanoindenter, G200 equipped with a Berkovich tip).

ASSOCIATED CONTENT

Supporting Information

Chemical vapor deposition set-up, TGA analysis, surface contact angle measurements, nano-indentation results, and peel-off test results. This material is available free of charge via the Internet at http://pubs.acs.org.

AUTHOR INFORMATION

Corresponding Author

*E-mail: sreekumarannair@aims.amrita.edu.

Notes

The authors declare no competing financial interest.

ACKNOWLEDGMENTS

V.A.G acknowledges a Ph.D. research fellowship from National University of Singapore. S.S.D acknowledges the A*STAR Graduate Academy for providing him the A*STAR Graduate scholarship for his Ph.D. study. The authors thank Mr. E. Naveen Kumar for his contributions. The authors also gratefully acknowledge the financial support from M3TC (Economic Development Board), Singapore (Grant R-26-501-018-414).

REFERENCES

(1) Guo, Z.; Liu, W.; Su, B.-L. *J. Colloid Interface Sci.* **2011**, *353* (2), 335−355.
(2) Ganesh, V. A.; Raut, H. K.; Nair, A. S.; Ramakrishna, S. *J. Mater.Chem.* **2011**, *21*, 16304−16322.
(3) Chhatre, S. S.; Tuteja, A.; Choi, W.; Revaux, A.; Smith, D.; Mabry, J. M.; McKinley, G. H.; Cohen, R. E. *Langmuir* **2009**, *25*, 13625−13632.
(4) Choi, W.; Tuteja, A.; Chhatre, S.; Mabry, J. M.; Cohen, R. E.; McKinley, G. H. *Adv. Mater.* **2009**, *21*, 2190−2195.
(5) Misra, R.; Cook, R. D.; Morgan, S. E. *J. Appl. Polym. Sci.* **2010**, *115*, 2322−2331.
(6) Muthiah, P.; Hsu, S.-H.; Sigmund, W. *Langmuir* **2010**, *26*, 12483−12487.
(7) Yan, Y. Y.; Gao, N.; Barthlott, W. *Adv. Colloid Interface Sci.* **2011**, *169*, 80−105.
(8) Nishimoto, S.; Kubo, A.; Zhang, X.; Liu, Z.; Taneichi, N.; Okui, T.; Murakami, T.; Komine, T.; Fujishima, A. *Appl. Surf. Sci.* **2008**, *254*, 5891−5894.
(9) Katsumata, K.-i.; Cordonier, C. E. J.; Shichi, T.; Fujishima, A. *Mater. Sci. Eng., B* **2010**, *173*, 267−270.
(10) Nakata, K.; Udagawa, K.; Ochiai, T.; Sakai, H.; Murakami, T.; Abe, M.; Fujishima, A. *Mater. Chem. Phys.* **2011**, *126*, 484−487.
(11) Fujishima, A.; Rao, T. N.; Tryk, D. A. *J. Photochem. Photobiol., C* **2000**, *1*, 1−21.
(12) Parkin, I. P.; Palgrave, R. G. *J. Mater.Chem.* **2005**, *15*, 1689−1695.
(13) Wang, X.; Ding, B.; Yu, J.; Wang, M. *Nano Today* **2011**, *6*, 510−530.
(14) Levkin, P. A.; Svec, F.; Fréchet, J. M. J. *Adv. Funct. Mater.* **2009**, *19*, 1993−1998.
(15) Ganesh, V. A.; Nair, A. S.; Raut, H. K.; Yuan Tan, T. T.; He, C.; Ramakrishna, S.; Xu, J. *J. Mater.Chem.* **2012**, *22*, 18479−18485.
(16) Zhang, Y.-L.; Xia, H.; Kim, E.; Sun, H.-B. *Soft Matter* **2012**, *8*, 11217−11231.
(17) Qu, M.; Zhang, B.; Song, S.; Chen, L.; Zhang, J.; Cao, X. *Adv. Funct. Mater.* **2007**, *17*, 593−596.

(18) Wang, D.; Guo, Z.; Chen, Y.; Hao, J.; Liu, W. *Inorg. Chem.* **2007**, *46*, 7707−7709.
(19) Zou, L.; Xiang, X.; Fan, J.; Li, F. *Chem.Mater.* **2007**, *19*, 6518−6527.
(20) Dunnill, C. W.; Page, K.; Aiken, Z. A.; Noimark, S.; Hyett, G.; Kafizas, A.; Pratten, J.; Wilson, M.; Parkin, I. P. *J. Photochem. Photobiol. A* **2011**, *220*, 113−123.
(21) Liu, H.; Szunerits, S.; Pisarek, M.; Xu, W.; Boukherroub, R. *ACS Appl. Mater. Interfaces* **2009**, *1*, 2086−2091.
(22) Zhang, J.; Pu, G.; Severtson, S. J. *ACS Appl. Mater. Interfaces* **2010**, *2*, 2880−2883.
(23) Kitagawa, D.; Kobatake, S. *Chem. Sci.* **2012**, *3* (5), 1445−1449.
(24) Nishimoto, S.; Kubo, A.; Nohara, K.; Zhang, X.; Taneichi, N.; Okui, T.; Liu, Z.; Nakata, K.; Sakai, H.; Murakami, T.; Abe, M.; Komine, T.; Fujishima, A. *Appl. Surf. Sci.* **2009**, *255*, 6221−6225.
(25) Li, Y.; Sasaki, T.; Shimizu, Y.; Koshizaki, N. *Small* **2008**, *4*, 2286−2291.
(26) Li, Y.; Sasaki, T.; Shimizu, Y.; Koshizaki, N. *J. Am. Chem. Soc.* **2008**, *130*, 14755−14762.
(27) Prado, R.; Beobide, G.; Marcaide, A.; Goikoetxea, J.; Aranzabe, A. *Sol. Energy Mater. Sol. Cells* **2010**, *94*, 1081−1088.
(28) Bedford, N. M.; Steckl, A. *J ACS Appl. Mater. Interfaces* **2010**, *2*, 2448−2455.
(29) Cassie, A. B. D.; Baxter, S. *Trans. Faraday Soc.* **1944**, *40*, 546−551.
(30) Byun, D.; Hong, J.; Saputra, Ko, J. H.; Lee, Y. J.; Park, H. C.; Byun, B.-K.; Lukes, J. R. *J. Bionic Eng.* **2009**, *6*, 63−70.
(31) Luo, Z. Z.; Zhang, Z. Z.; Hu, L. T.; Liu, W. M.; Guo, Z. G.; Zhang, H. J.; Wang, W. J. *Adv. Mater.* **2008**, *20*, 970−974.
(32) Otten, A.; Herminghaus, S. *Langmuir* **2004**, *20*, 2405−2408.
(33) Xie, Q.; Xu, J.; Feng, L.; Jiang, L.; Tang, W.; Luo, X.; Han, C. C. *Adv. Mater.* **2004**, *16* (4), 302−305.
(34) Wang, X.; Liu, X.; Zhou, F.; Liu, W. *Chem. Commun.* **2011**, *47* (8), 2324−2326.
(35) He, Z.; Ma, M.; Lan, X.; Chen, F.; Wang, K.; Deng, H.; Zhang, Q.; Fu, Q. *Soft Matter* **2011**, *7* (14), 6435−6443.
(36) Wang, X.; Hu, H.; Ye, Q.; Gao, T.; Zhou, F.; Xue, Q. *J. Mater.Chem.* **2012**, *22* (19), 9624−9631.
(37) Ganesh, V. A.; Dinachali, S. S.; Raut, H. K.; Walsh, T. M.; Nair, A. S.; Ramakrishna, S. *RSC Adv.*, DOI:10.1039/C3RA22968H.
(38) Deng, X.; Mammen, L.; Butt, H.-J.; Vollmer, D. *Science* **2012**, *335*, 67−70.
(39) Xiong, D.; Liu, G.; Hong, L.; Duncan, E. J. S. *Chem.Mater.* **2011**, *23*, 4357−4366.
(40) Tuteja, A.; Choi, W.; Ma, M. L.; Mabry, J. M.; Mazzella, S. A.; Rutledge, G. C.; McKinley, G. H.; Cohen, R. E. *Science* **2007**, *318*, 1618−1622.
(41) Tuteja, A.; Choi, W.; Mabry, J. M.; McKinley, G. H.; Cohen, R. E. *Proc. Natl. Acad. Sci. U.S.A.* **2008**, *105*, 18200−18205.
(42) Cao, L.; Price, T. P.; Weiss, M.; Gao, D. *Langmuir* **2008**, *24*, 1640−1643.
(43) Rajendra Kumar, R. T.; Mogensen, K. B.; Bøggild, P. *J. Phys. Chem. C* **2010**, *114*, 2936−2940.
(44) Xi, J. M.; Feng, L.; Jiang, L. *Appl. Phys. Lett.* **2008**, *92*, 053102.
(45) Wu, W.; Wang, X.; Wang, D.; Chen, M.; Zhou, F.; Liu, W.; Xue, Q. *Chem. Commun.* **2009**, 1043−1045.
(46) Butt, H.-J.; Semprebon, C.; Papadopoulos, P.; Vollmer, D.; Brinkmann, M.; Ciccotti, M. *Soft Matter* **2013**, *9*, 418−428.
(47) Hsieh, C.-T.; Chen, J.-M.; Kuo, R.-R.; Lin, T.-S.; Wu, C.-F. *Appl. Surf. Sci.* **2005**, *240* (1−4), 318−326.
(48) Steele, A.; Bayer, I.; Loth, E. *Nano Lett.* **2008**, *9* (1), 501−505.
(49) Xue, Z.; Liu, M.; Jiang, L. *J. Polym. Sci., Part B: Polym. Phys.* **2012**, *50* (17), 1209−1224.
(50) Nair, A. S.; Shengyuan, Y.; Peining, Z.; Ramakrishna, S. *Chem.Commun.* **2010**, *46*, 7421−7423.
(51) Shengyuan, Y.; Peining, Z.; Nair, A. S.; Ramakrishna, S. *J. Mater.Chem.* **2011**, *21*, 6541−6548.
(52) Nair, A. S.; Jose, R.; Shengyuan, Y.; Ramakrishna, S. *J. Colloid Interface Sci.* **2011**, *353*, 39−45.
(53) Peining, Z.; Nair, A. S.; Shengjie, P.; Shengyuan, Y.; Ramakrishna, S. *ACS Appl. Mater. Interfaces* **2012**, *4* (2), 581−585.
(54) Peining, Z.; Nair, A. S.; Shengyuan, Y.; Shengjie, P.; Elumalai, N. K.; Ramakrishna, S. *J. Photochem. Photobiol., A* **2012**, *231* (1), 9−18.
(55) Dinachali, S. S.; Saifullah, M. S. M.; Ganesan, R.; Thian, E. S.; He, C. *Adv. Funct. Mater.* DOI: 10.1002/adfm.201202577.
(56) Ganesan, R.; Dinachali, S. S.; Lim, S. H.; Saifullah, M. S. M.; Chong, W. T.; Lim, A. H. H.; Yong, J. J.; Thian, E. S.; He, C.; Low, H.Y. *Nanotechnology* **2012**, *23*, 315304.
(57) Ganesh, V. A.; Nair, A. S.; Raut, H. K.; Walsh, T. M.; Ramakrishna, S. *RSC Adv.* **2012**, *2*, 2067−2072.
(58) *J. Phys. Chem. Ref. Data* **1982**, *11* (Supplement 2).